

# Encapsulation of Functional Moieties within Branched Star Polymers: Effect of Chain Length and Solvent on Site Isolation

Stefan Hecht, Nikolay Vladimirov, and Jean M. J. Fréchet\*

Contribution from the Department of Chemistry, University of California, Berkeley, California 94720-1460

Received September 7, 2000

**Abstract:** Porphyrin and pyrene photoactive cores have been encapsulated within an isolating polymeric shell using an efficient and general strategy based on the use of dendritic initiators for the ring-opening polymerization of  $\epsilon$ -caprolactone to yield functional core star polymers. The isolation of the core functionalities has been studied using fluorescence quenching and fluorescence resonance energy transfer (FRET) techniques as well as solvatochromic probes. With increasing chain length as well as solvent polarity, enhanced site isolation of the core has been observed. These findings have been correlated to actual molecular dimensions independently measured by pulsed field gradient spin-echo (PGSE) NMR. The developed synthetic methodology offers a rapid route to efficient encapsulation of functional moieties and therefore has potential for the design of new materials.

## Introduction

In recent years, one of the major objectives in dendrimer chemistry<sup>1</sup> has been the encapsulation of active core functionalities within dendritic backbones.<sup>2</sup> Numerous examples of such structures have shown profound effects of the dendrimer shell on the core properties, and impressively demonstrated the importance of this site isolation concept.<sup>3</sup> The use of dendritic nonnatural building blocks to mimic enzyme functions<sup>4</sup> will ultimately provide a more detailed understanding of biological processes, and facilitate the design of artificial nanoscale molecular devices by creating specific microenvironments around active units.<sup>5</sup> Porphyrin core dendrimers<sup>6</sup> have received special attention due to their potential as heme protein mimics for electron transport,<sup>6a–f</sup> dioxygen binding,<sup>6g,h</sup> and oxidation catalysis.<sup>6i,j</sup>

The preparation of structurally perfect dendrimers traditionally suffers from its time-consuming nature due to the required repetitive coupling and activation steps, and the necessity for extensive purification. Although accelerated synthetic protocols<sup>7</sup> and the construction of less perfect analogues<sup>8</sup> have been

successfully implemented, the synthesis of highly branched structures having exotic core functionalities remains challenging.

(1) (a) Newkome, G. R.; Moorefield, C. N.; Vögtle, F. *Dendritic Molecules: Concepts, Synthesis, Perspectives*; VCH: Weinheim, 1996. (b) Bosman, A. W.; Jansen, H. M.; Meijer, E. W. *Chem. Rev.* **1999**, *99*, 1665. (c) Fischer, M.; Vögtle, F. *Angew. Chem., Int. Ed.* **1999**, *38*, 885. (d) Matthews, O. A.; Shipway, A. N.; Stoddart, J. F. *Prog. Polym. Sci.* **1998**, *23*, 1. (e) Fréchet, J. M. J.; Hawker, C. J. In *Comprehensive Polymer Science*, 2nd Suppl.; Aggarwal, S. L., Russo, S., Eds.; Pergamon Press: Oxford, 1996; p 140. (f) Fréchet, J. M. J. *Science*, **1994**, *263*, 1710. (g) Tomalia, D. A.; Naylor, A. M.; Goddard, W. A., III *Angew. Chem., Int. Ed.* **1990**, *29*, 138.

(2) Functional dendrimers have been comprehensively reviewed by: (a) Chow, H.-F.; Mong, T. K.-K.; Nongrum, M. F.; Wan, C.-W. *Tetrahedron* **1998**, *54*, 8543. Other reviews include: (b) Newkome, G. R.; He, E.; Moorefield, C. N. *Chem. Rev.* **1999**, *99*, 1689. (c) Archut, A.; Vögtle, F. *Chem. Soc. Rev.* **1999**, *27*, 233.

(3) Hecht, S.; Fréchet, J. M. J. *Angew. Chem., Int. Ed.* **2001**, *40*, 74.

(4) Dendrimers as biological mimics have been reviewed in: Smith, D. K.; Diederich, F. *Chem. Eur. J.* **1998**, *4*, 1353.

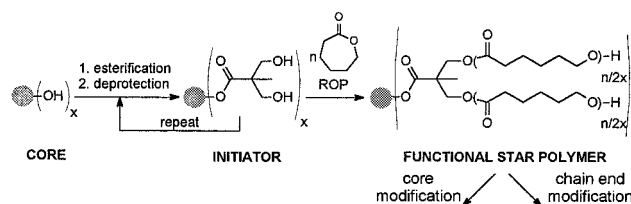
(5) (a) Wang, P.-W.; Liu, Y.-J.; Devadoss, C.; Bharathi, P.; Moore, J. S. *Adv. Mater.* **1996**, *8*, 237. (b) Kawa, M.; Fréchet, J. M. J. *Chem. Mater.* **1998**, *10*, 286. (c) Halim, M.; Pillow, J. N. G.; Samuel, I. D. W.; Burn, P. L. *Adv. Mater.* **1999**, *11*, 371. (d) Freeman, A. W.; Koene, S. C.; Malenfant, P. R. L.; Thompson, M. E.; Fréchet, J. M. J. *J. Am. Chem. Soc.* In press.

(6) (a) Dandliker, P. J.; Diederich, F.; Gross, M.; Knobler, C. B.; Louati, A.; Sanford, E. M. *Angew. Chem., Int. Ed.* **1994**, *33*, 1739. (b) Dandliker, P. J.; Diederich, F.; Gisselbrecht, J.-P.; Louati, A.; Gross, M. *Angew. Chem., Int. Ed.* **1995**, *34*, 2725. (c) Sadamoto, R.; Tomioka, N.; Aida, T. *J. Am. Chem. Soc.* **1996**, *118*, 3978. (d) Dandliker, P. J.; Diederich, F.; Zingg, A.; Gisselbrecht, J.-P.; Gross, M.; Louati, A.; Sanford, E. M. *Helv. Chim. Acta* **1997**, *80*, 1773. (e) Pollak, K. W.; Leon, J. W.; Fréchet, J. M. J.; Maskus, M.; Abruña, H. D. *Chem. Mater.* **1998**, *10*, 30. (f) Weyermann, P.; Gisselbrecht, J.-P.; Boudon, C.; Diederich, F.; Gross, M. *Angew. Chem., Int. Ed.* **1999**, *38*, 3215. (g) Jiang, D.-L.; Aida, T. *Chem. Commun.* **1996**, 1523. (h) Collman, J. P.; Fu, L.; Zingg, A.; Diederich, F. *Chem. Commun.* **1997**, 193. (i) Bhyrappa, P.; Young, J. K.; Moore, J. S.; Suslick, K. S. *J. Am. Chem. Soc.* **1996**, *118*, 5708. (j) Bhyrappa, P.; Young, J. K.; Moore, J. S.; Suslick, K. S. *J. Mol. Catal. A* **1996**, *113*, 109. For additional work on porphyrin core dendrimers see: (k) Jin, R.-H.; Aida, T.; Inoue, S. *J. Chem. Soc., Chem. Commun.* **1993**, 1260. (l) Tomoyose, Y.; Jiang, D.-L.; Jin, R.-H.; Aida, T.; Yamashita, T.; Horie, K.; Yashima, E.; Okamoto, Y. *Macromolecules* **1996**, *29*, 5236. (m) Pollak, K. W.; Sanford, E. M.; Fréchet, J. M. J. *J. Mater. Chem.* **1998**, *8*, 519. (n) Jiang, D.-L.; Aida, T. *J. Am. Chem. Soc.* **1998**, *120*, 10895. (o) Bhyrappa, P.; Vijayanthimala, G.; Suslick, K. S. *J. Am. Chem. Soc.* **1999**, *121*, 262. (p) Kimura, M.; Shiba, T.; Muto, T.; Hanabusa, K.; Shirai, H. *Macromolecules* **1999**, *32*, 8237. (q) Vinogradov, S. A.; Lo, L.-W.; Wilson, D. F. *Chem. Eur. J.* **1999**, *5*, 1338. (r) Vinogradov, S. A.; Wilson, D. F. *Chem. Eur. J.* **2000**, *6*, 2456. (s) Matos, M. S.; Hofkens, J.; Verheijen, W.; De Schryver, F. C.; Hecht, S.; Pollak, K. W.; Fréchet, J. M. J.; Forier, B.; Dehaen, W. *Macromolecules* **2000**, *33*, 2967.

(7) Accelerated growth strategies have been reported. For double-stage convergent growth approaches, see: (a) Wooley, K. L.; Hawker, C. J.; Fréchet, J. M. J. *J. Am. Chem. Soc.* **1991**, *113*, 4252. (b) Ihre, H.; Hult, A.; Fréchet, J. M. J.; Gitsov, I. *Macromolecules* **1998**, *31*, 4061. For a double exponential growth approach, consult: (c) Kawaguchi, T.; Walker, K. L.; Wilkins, C. L.; Moore, J. S. *J. Am. Chem. Soc.* **1995**, *117*, 2159. The use of "hypermonomer" building blocks is described in: (d) Wooley, K. L.; Hawker, C. J.; Fréchet, J. M. J. *Angew. Chem., Int. Ed.* **1994**, *33*, 82. (e) L'abbe, G.; Forier, B.; Dehaen, W. *J. Chem. Soc., Chem. Commun.* **1996**, 1262. Orthogonal monomers have been used by: (f) Spindler, R.; Fréchet, J. M. J. *J. Chem. Soc., Perkin Trans. 1* **1993**, 913. (g) Zeng, F.; Zimmerman, S. C. *J. Am. Chem. Soc.* **1996**, *118*, 5326. (h) Freeman, A. W.; Fréchet, J. M. J. *Org. Lett.* **1999**, *1*, 685.

(8) Recently, there have been major advances in achieving dendrimer-like properties using hyperbranched polymers. Although such materials are easily accessible via one-pot procedures, the covalent encapsulation of a single entity is not currently practical using this approach. Comprehensive reviews on hyperbranched polymers include: (a) Kim, Y. H. *J. Polym. Sci., Part A: Polym. Chem.* **1998**, *36*, 1685. (b) Voit, B. I. *Acta Polym.* **1995**, *46*, 87. (c) Reference 1e.

## Scheme 1



Recently, we overcame these synthetic obstacles by efficiently encapsulating porphyrins in a starlike polymer shell.<sup>9</sup> This strategy was based on the “living” ring-opening polymerization of  $\epsilon$ -caprolactone using multifunctional, highly branched porphyrin initiators. This very practical approach benefits from the rapid synthesis, the ease of purification, and the flexibility of post-modification of both core and chain ends.

Here we report on the generality and modularity of our synthetic route to encapsulate active core functionalities that enable us to use a variety of spectroscopic techniques to evaluate the degree of site-isolation of the core with regard to chain length as well as solvent. In particular, we utilize fluorescence resonance energy transfer (FRET) from terminal donor chromophores to a core acceptor dye as a suitable tool to study the conformational dynamics in such functional star polymer architectures. The chain length and solvent dependence of core encapsulation is supported by pulsed field gradient spin-echo (PGSE) NMR experiments, which allow a direct correlation with molecular size.

## Results and Discussion

**Synthesis.** Rapid encapsulation of a functional moiety involves the preparation of a low-generation hydroxyl-terminated aliphatic polyester dendritic initiator<sup>7b,10</sup> for the ring-opening polymerization of  $\epsilon$ -caprolactone<sup>11</sup> to afford the desired functional star polymers (Scheme 1). All polymerizations were carried out in the bulk employing catalytic amounts of tin(II) 2-ethylhexanoate, as described in detail by Trollsås and Hedrick.<sup>12</sup> The desired polymers were obtained in essentially quantitative yields and narrow polydispersities after a single precipitation into methanol (Table 1). Molecular weights (MW) were easily controlled by adjusting the monomer-to-initiator ratio, in accord with the “living” nature of the polymerization. Increasing degree of polymerization (DP)<sup>13</sup> generally required longer polymerization times. Due to the limited solubility of the initiators in the monomer, polymers with DP > 25 were generally prepared most effectively.

We focused on porphyrin and pyrene cores due to their unique spectroscopic characteristics that allowed us to probe their microenvironment, and therefore to evaluate the degree of site isolation of the core. The use of tetrakis(4-hydroxyphenyl)porphyrin and tetrakis(3,5-dihydroxyphenyl)porphyrin having multiple reactive groups offers the advantage of rapidly generat-

Table 1. Molecular Weight Characteristics of Star Polymers

	DP <sub>(NMR)</sub>	$\bar{M}_n$ (NMR)	$\bar{M}_w/\bar{M}_n$ (GPC)
<b>1a</b>	26.6	25 400	1.14
<b>1b</b>	33.3	31 600	1.13
<b>1c</b>	44.6	41 800	1.17
<b>1d</b>	54.2	50 600	1.19
<b>2a</b>	24.9	47 200	1.18
<b>2b</b>	31.9	59 900	1.14
<b>2c</b>	41.0	76 600	1.12
<b>2d</b>	50.4	93 700	1.10
<b>3a</b>	24.9	50 000	1.18
<b>3b</b>	31.9	62 700	1.14
<b>3c</b>	41.0	79 400	1.12
<b>3d</b>	50.4	96 500	1.10
<b>7a</b>	33.7	8 000	1.35
<b>7b</b>	56.8	13 300	1.37
<b>7c</b>	84.5	19 600	1.32
<b>7d</b>	116.3	26 900	1.26
<b>8a</b>	31.5	14 700	1.21
<b>8b</b>	53.6	24 800	1.17
<b>8c</b>	82.4	38 000	1.16
<b>8d</b>	107.3	49 300	1.18

ing many initiating sites. Therefore, first generation dendrimers having 8 and 16 hydroxyl functionalities, respectively, were used as initiators to grow 8-arm and 16-arm stars. Metalation of the obtained polymers gave two series of zinc porphyrin star polymers **1a–d**<sup>14</sup> and **2a–d** that were used in fluorescence quenching studies employing an external probe (Scheme 2). In contrast, esterification of the polymer chain ends using coumarin-3-carboxylic acid chloride provided star polymers **3a–d** having an internal probe since the coumarin chromophores are capable of efficient FRET to the porphyrin core (Scheme 3). Dendrimer **3e** and coumarin-terminated star **4** having no porphyrin acceptor core were also prepared as model compounds for comparison purposes.

To complement the spectroscopic measurements on the porphyrin core star polymers as well as to demonstrate the generality of this encapsulation strategy, pyrene core star polymers **7a–d** and **8a–d** having either 2 or 4 arms were prepared from their respective initiators **5** and **6** (Scheme 4). The pyrene core is ideally suited for use as a solvatochromic probe since its fluorescence signal is highly sensitive toward the local environment as well as aggregation (excimer formation).

**Fluorescence Quenching Experiments.** In our initial communication,<sup>9</sup> we used the interaction of a small molecule fluorescence quencher such as methyl viologen with the interior zinc porphyrin to evaluate the core accessibility in stars **1a–d** and **2a–d** (Scheme 2). The products of the quenching rate constant  $k_q$  and the excited-state lifetime  $\tau$  were determined as a function of chain length, i.e., degree of polymerization (DP), using Stern–Volmer analysis<sup>15</sup> (Figure 1). A direct evaluation of  $k_q$  to measure core accessibility is possible since the absorption and fluorescence spectra as well as the fluorescence quantum yields (in the absence of the quencher) remain essentially constant, indicating no significant change of  $\tau$ .<sup>16</sup>

A strong shielding of the core moiety in the star polymers compared to zinc tetraphenylporphyrin (ZnTPP) as the reference

(9) Hecht, S.; Ihre, H.; Fréchet, J. M. J. *J. Am. Chem. Soc.* **1999**, *121*, 9239.

(10) (a) Ihre, H.; Hult, A.; Söderlind, E. *J. Am. Chem. Soc.* **1996**, *118*, 6388.

(11) For a recent review, consult: Löfgren, A.; Albertsson, A.-C.; Dubois, P.; Jérôme, R. *J. Macromol. Sci., Rev. Macromol. Chem. Phys.* **1995**, *C35*, 379.

(12) (a) Trollsås, M.; Hedrick, J. L.; Mecerreyes, D.; Dubois, P.; Jérôme, R.; Ihre, H.; Hult, A. *Macromolecules* **1997**, *300*, 8508. (b) Trollsås, M.; Hedrick, J. L.; Mecerreyes, D.; Dubois, P.; Jérôme, R.; Ihre, H.; Hult, A. *Macromolecules* **1998**, *31*, 2756. (c) Trollsås, M.; Hedrick, J. L. *J. Am. Chem. Soc.* **1998**, *120*, 4644 and references therein.

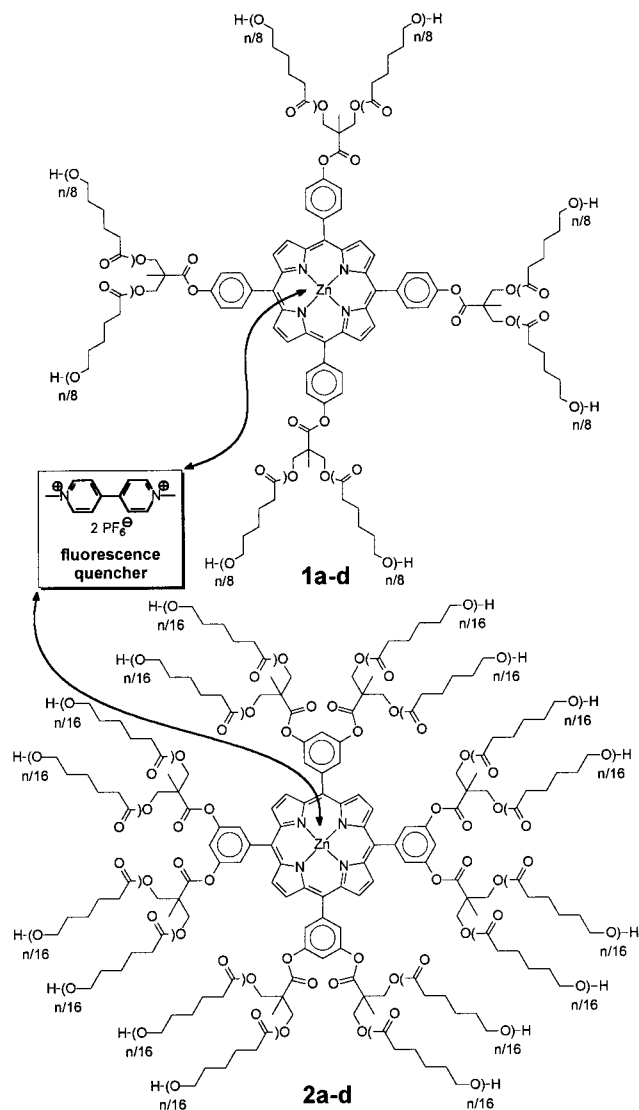
(13) Values given in Table 1 refer to the average DP of individual chains, as indicated in Schemes 1–4.

(14) In all described polymer series, the index a–d indicates increasing DP. See Table 1 for further details.

(15) Consult standard photochemistry textbooks: (a) Turro, N. J. *Modern Molecular Photochemistry*; University Science Books: Sausalito, 1991. (b) Gilbert, A.; Baggott, J. *Essentials of Molecular Photochemistry*; CRC Press: Boca Raton, 1991. (c) Klessinger, M.; Michl, J. *Excited States and Photochemistry of Organic Molecules*; VCH: Weinheim, 1995.

(16) Turro, N. J.; Barton, J. K.; Tomalia, D. A. *Acc. Chem. Res.* **1991**, *24*, 332.

Scheme 2

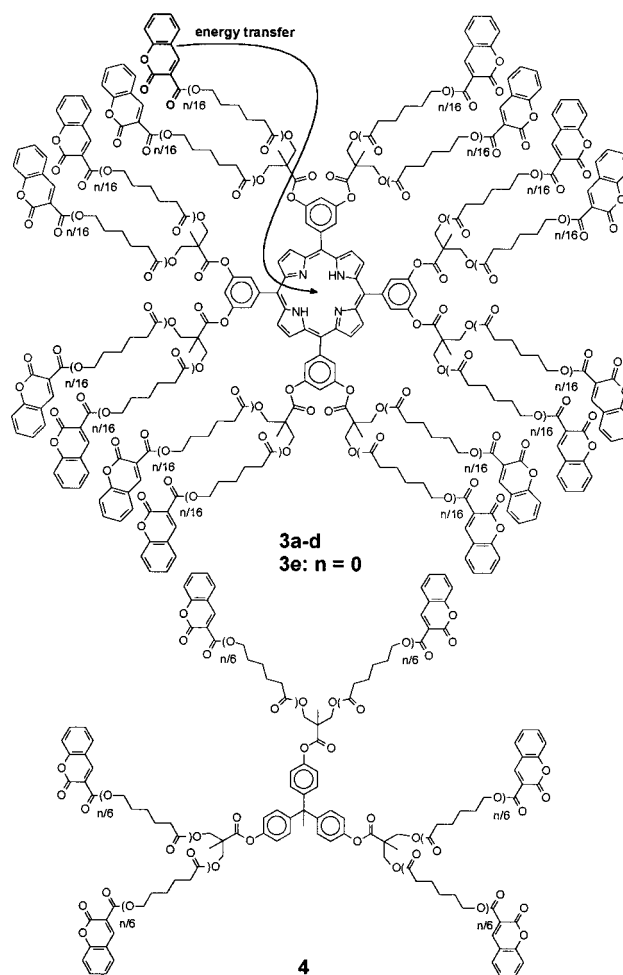


was observed, thereby demonstrating inhibited penetration of the small molecule quencher through the polymeric backbone. The magnitude of site isolation is significantly higher than that in the dendritic counterparts employed in similar quenching studies.<sup>6e,k</sup> The degree of shielding is clearly dependent on the chain length: with increasing DP the accessibility of the core decreases. Extrapolation suggests a rather steep decline in core accessibility in the early stages where DP is less than 25. Surprisingly, the quenching efficiency is comparable for 8-arm and 16-arm stars having similar DPs, suggesting that the chain length, rather than the number of arms, is crucial for isolation of the core unit. This finding is in agreement with existing experimental studies<sup>17</sup> as well as theoretical models describing the shape of star polymers using an asphericity factor  $\delta$  that has a value of 1 for cylindrical molecules and vanishes for molecules with spherical symmetry.<sup>18</sup> In good solvents, only minor differences are predicted between the 8-arm star ( $\delta = 0.14$ )<sup>19</sup> and 16-arm star ( $\delta = 0.07$ ), and this difference is

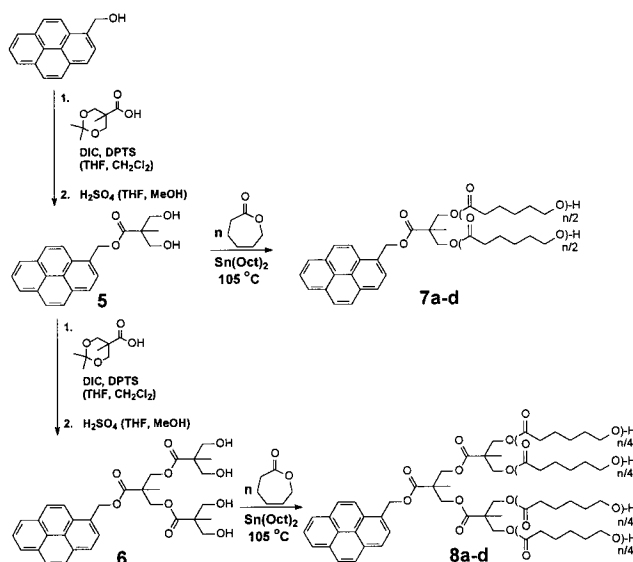
(17) (a) Willner, L.; Jucknischeke, O.; Richter, D.; Farago, B.; Fetters, L. J.; Huang, J. S. *Europhys. Lett.* **1992**, *19*, 297. (b) Willner, L.; Jucknischeke, O.; Richter, D.; Roovers, J.; Zhou, L.-L.; Topowski, P. M.; Fetters, L. J.; Huang, J. S.; Lin, M. Y.; Hadjichristidis *Macromolecules* **1994**, *27*, 3821.

(18) (a) Rudnick, J.; Gaspari, G. *J. Phys. A* **1986**, *19*, L191. (b) Aronowitz, J. A.; Nelson, D. R. *J. Phys.* **1986**, *47*, 1445.

Scheme 3



Scheme 4



expected to be diminished even further in poor solvents,<sup>20</sup> such as the acetonitrile employed in this experiment.

However, the fluorescence quenching experiments were somewhat limited due to the low solubility of the external probe

(19) Calculated by using  $\delta = (150f^{-1} - 140f^{-2}) / (135 - 120f^{-1} - 4f^{-2})$ , where  $f$  is the number of arms. For further details, consult: Wei, G.; Eichinger, B. E. *J. Chem. Phys.* **1990**, *93*, 1430.

(20) Sikorski, A.; Romiszowski, P. *J. Chem. Phys.* **1998**, *109*, 6169.

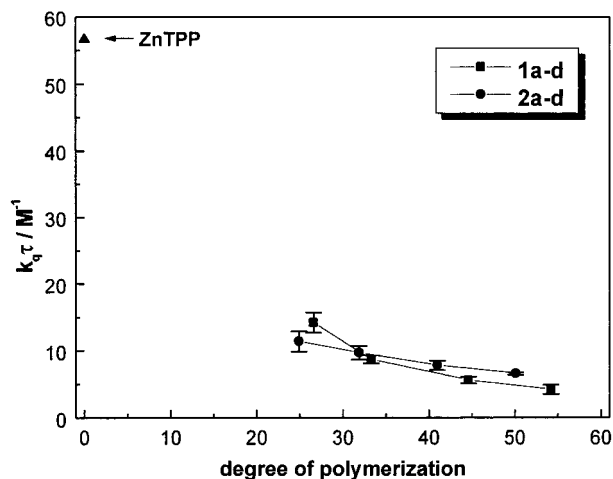


**Figure 1.** Fluorescence quenching for two series of zinc porphyrin star polymers having 8 arms (**1a–d**) and 16 arms (**2a–d**). The  $k_q\tau$  values are derived from Stern–Volmer analysis in acetonitrile employing methyl viologen as the quencher.

in the less polar solvents that are good solvents for the investigated polymers. Rather than employing different neutral quenchers,<sup>6k,q</sup> we sought to take advantage of the unique design of the system with its multiple reactive chain ends to attach an internal probe enabling the study of site isolation as a function of solvent.

**FRET Studies.** FRET involves the nonradiative transfer of singlet excitation energy from a donor chromophore to an acceptor chromophore. According to Förster's mechanism,<sup>21a</sup> the magnitude of the interaction, i.e., the FRET efficiency ( $\Phi_{\text{FRET}}$ ), is inversely proportional to the sixth power of the donor–acceptor separation.<sup>13,21</sup> Mainly due to this sensitive distance dependence, FRET has proven to be an exceptional tool for the study of the conformation and motion of biological macromolecules.<sup>22</sup> To monitor interactions over the range of several nanometers, a high intrinsic probability of FRET and therefore maximized spectral overlap between the emission of the donor and the absorption of the acceptor is required.<sup>13,21</sup>

In the present study, the porphyrin core served as acceptor, whereas multiple donors were introduced by modification of the chain ends (Scheme 3). In our system, coumarin-3-carboxylates were chosen as the donor chromophores since their emission centered around 420 nm strongly overlaps with the Soret absorption band ( $\lambda_{\text{max}} = 420$  nm) of the porphyrin acceptor core (Figure 2).<sup>23</sup> In addition, coumarin-3-carboxylic acid is a commercially available, rather inexpensive dye that can be conveniently linked to the hydroxyl-chain ends via esterification.<sup>9</sup> When the coumarin donors in polymers **3a–d** were excited selectively ( $\lambda_{\text{exc}} = 350$  nm), emission from both the coumarins and the porphyrin acceptor was observed, demon-

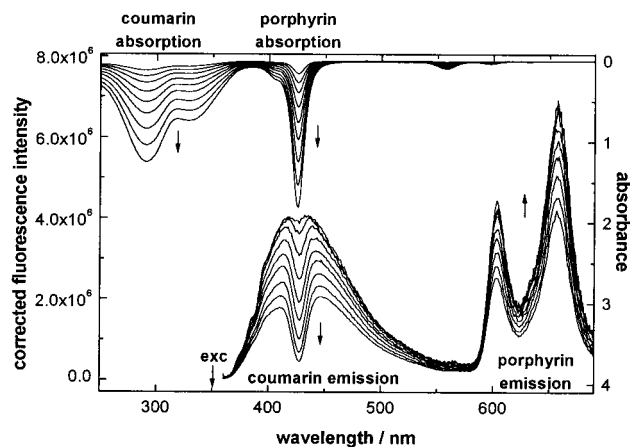


**Figure 2.** Photophysical characteristics of compounds **3** in chloroform. Increasing optical density (concentrations: 0.2–4  $\mu\text{M}$ ) of the sample (top) leads to enhanced self-absorption (trivial energy transfer) in the system as indicated by the shape of the donor emission spectrum (bottom).

strating that FRET was facile but not quantitative in this system. In a separate control experiment, excitation of a porphyrin core star polymer having no coumarin donor chromophores attached led to no observable emission due to the negligible absorption at this particular excitation wavelength. It is important to note that at concentrations above 0.2 mM, the extremely high extinction coefficient of the Soret band ( $\epsilon = 519\,000\text{ M}^{-1}\text{ cm}^{-1}$ ) promotes self-absorption, i.e., trivial radiative energy transfer. Since the coumarin emission spectrum is very indicative of this effect (Figure 2), it could be shown that the portion of the radiative energy transfer increased linearly with increasing concentration and therefore optical density, assuming constant efficiency of the nonradiative transfer, i.e., FRET. In all experiments concentrations of approximately 0.1 mM were employed to avoid this self-absorption process, and to enable the use of both good and poor solvents in the experiments. On the basis of the very low concentrations employed, aggregation phenomena are unlikely to occur. Further experimental evidence for this assumption arises from the excellent agreement of the MW determined independently by light scattering and <sup>1</sup>H NMR as well as the constant gel permeation chromatography (GPC) elution volume of polymers **3a–d** within a wide concentration range ( $10^{-8}$ – $10^{-4}$  M in THF and  $\text{CHCl}_3$ ). The exclusion of aggregation is essential since only intramolecular FRET provides valuable information about the intrinsic polymer dynamics.

The dependence of FRET on polymer chain length was investigated (Figure 3). As the chain length increases and the donor chromophores are placed at further average distances from the acceptor core, the donor emission intensity increases as the result of the reduced probability of FRET in the system. In one extreme case, quantitative FRET is observed in **3e** due to extremely short average donor–acceptor distances. In contrast, no FRET occurs in **4** as a result of the absence of an acceptor chromophore.

The values of  $\Phi_{\text{FRET}}$  were determined by the method of quenched donor emission,<sup>24</sup> which compares the coumarin emission in the presence of the acceptor (**3a–e**) to the emission in the absence of an acceptor, as in model compound **4**.<sup>25</sup> The results shown in Figure 4 obtained with different solvents reflect the chain length dependence, as described above, and complement our earlier findings using fluorescence quenching (vide supra). Interestingly, a pronounced solvent effect is observed. In good solvents for the poly( $\epsilon$ -caprolactone) stars, such as  $\text{CHCl}_3$  or toluene, a steep decline of  $\Phi_{\text{FRET}}$  is observed with

(21) (a) Förster, T. *Fluoreszenz Organischer Verbindungen*; Vandenhoeck and Ruprecht: Göttingen, 1951. (b) Van der Meer, W. B.; Coker, G., III; Chen, S.-Y. *Resonance Energy Transfer, Theory and Data*; VCH: Weinheim, 1994.

(22) Representative recent reviews are given in the following: (a) Weiss, S. *Science* **1999**, *283*, 1676. (b) Szöllösi, J.; Damjanovich, S.; Mátyus, L. *Cytometry* **1998**, *34*, 159.

(23) To our knowledge, this is the first time the emission originating from a coumarin dye is quenched by the porphyrin Soret absorption. One example of energy transfer from a coumarin donor (7-diethylaminocoumarin-3-carboxylate) to a metalloporphyrin acceptor (palladium(II) tetraarylporphyrin) has been reported by: Kaschak, D. M.; Lean, J. T.; Waraksa, C. C.; Saupé, G. B.; Usami, H.; Mallouk, T. E. *J. Am. Chem. Soc.* **1999**, *121*, 3435. However, due to the red-shifted emission of the employed coumarin, sensitization of the Q-band and not the Soret band of the metalloporphyrin most likely occurred.

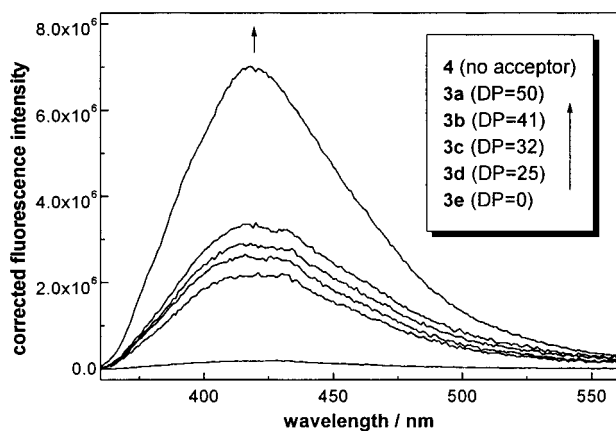


**Figure 3.** Corrected emission of the terminal coumarin donor chromophores in compounds **3a–e** and model compound **4** in chloroform as a function of chain length (DP).

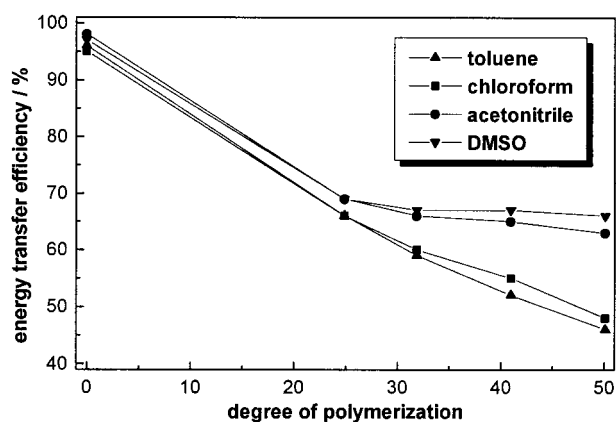


**Figure 4.** Resonance energy transfer from the terminal coumarin donor chromophores to the free-base porphyrin core acceptor in compounds **3a–e** employing different solvents. The energy transfer efficiencies were determined from the amount of quenched donor emission as compared to model compound **4**.

increasing DP, whereas in poor solvents, such as acetonitrile or DMSO,  $\Phi_{\text{FRET}}$  levels off at high DP. Although other coumarins such as 7-methoxycoumarin display solvent-dependent emission characteristics,<sup>26</sup> the observed effect is clearly due to conformational changes since the chain length is the only variable for measurements in each solvent.

We suggest that the collapse of star polymers **3** in poor solvents leads to a reduced *average* donor–acceptor distance and therefore increased  $\Phi_{\text{FRET}}$  as compared to the extended conformations present in good solvents (Figure 5).<sup>27</sup> In a crude approximation, the different slopes in Figure 4 can be rationalized by considering a sphere ( $\delta = 0.07$ , vide supra) for which the volume is directly related to the third power of the radius, i.e.,  $V \propto r^3$ . By progressing outward and assuming a similar

(24) We recently found this method to be well suited for studying FRET in dendritic systems: (a) Adronov, A.; Gilat, S.; Fréchet, J. M. J.; Ohta, K.; Neuwahl, F. V. R.; Fleming, G. R. *J. Am. Chem. Soc.* **2000**, *122*, 1175. (b) Gilat, S. L.; Adronov, A.; Fréchet, J. M. J. *Angew. Chem., Int. Ed.* **1999**, *38*, 1422. (c) Adronov, A.; Malenfant, P. R. L.; Fréchet, J. M. J. *Chem. Mater.* **2000**, *12*, 1463. For a detailed discussion, see also: Devadoss, C.; Bharati, P.; Moore, J. S. *J. Am. Chem. Soc.* **1996**, *118*, 9635. Quantifying the enhanced acceptor emission was found to be associated with a much greater error arising from the almost negligible emission of the model compound having no donors chromophores.

(25) Almost identical results were obtained using different model compounds such as methyl coumarin-3-carboxylate.

(26) (a) Seixas de Melo, J. S.; Becker, R. S.; Macanita, A. L. *J. Phys. Chem.* **1994**, *98*, 6054. (b) Schade, B.; Hagen, V.; Schmidt, R.; Herbrich, R.; Krause, E.; Eckardt, T.; Bendig, J. *J. Org. Chem.* **1999**, *64*, 9109.

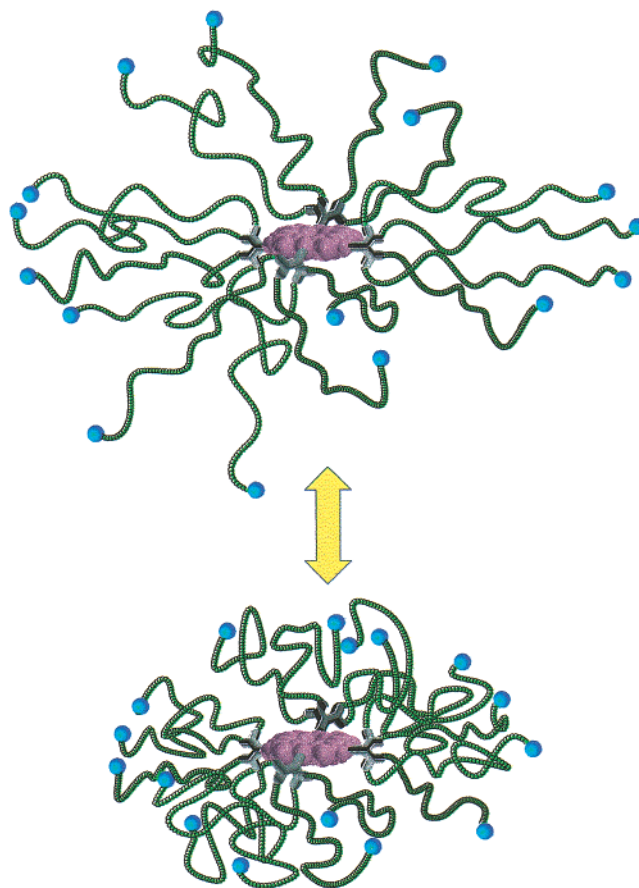


**Figure 5.** Illustration of the solvation induced encapsulation of the core functionality. While the polymer adopts a more extended conformation in a good solvent (top), it collapses in a poor solvent (bottom) leading to a reduced *average* donor–acceptor distance and therefore enhanced energy transfer efficiency. The terminal coumarin chromophores are shown in cyan, the poly(caprolactone) backbone in green, the dendritic branching unit in gray, and the porphyrin core in magenta.

density, the same changes in volume will be associated with smaller and smaller changes in radius. This behavior should be most pronounced in the solvent collapsed and therefore more densely packed structure since an increase in DP will have only a minor effect on the average donor–acceptor separation.

Recent work on dendritic systems with nearly quantitative  $\Phi_{\text{FRET}}$  ( $\Phi_{\text{FRET}} = 0.93–0.98$ ) related interchromophoric distances estimated from molecular modeling to the rate of FRET measured by time-resolved techniques.<sup>24a</sup> In contrast, the star polymer counterparts studied here cover a much wider range of donor–acceptor distance and therefore  $\Phi_{\text{FRET}}$  ( $\Phi_{\text{FRET}} = 0.46–0.98$ ). In the special case when  $\Phi_{\text{FRET}}$  is 0.5, the corresponding distance known as the Förster radius  $R_0$  can be calculated from the spectral overlap of the participating chromophores.<sup>21</sup> Since theory validates the assumption that, in the absence of any favorable interactions between chain ends and inner building blocks,<sup>1f</sup> the terminal groups are located near the periphery,<sup>28</sup> this allows a rough correlation of molecular size with measured  $\Phi_{\text{FRET}}$ . For this particular system,  $R_0$  is calculated

(27) A similar result has been observed in a dendritic system having a water-soluble carboxylate-functionalized periphery and a palladium porphyrin core. Different quenching constants of molecular oxygen were found with varying pH of the medium suggesting conformational changes of the dendrimer backbone. See refs 6q,r for further details.

(28) (a) Grest, G. S.; Kremer, K.; Milner, S. T.; Witten, T. A. *Macromolecules* **1989**, *22*, 1904. (b) Li, H.; Witten, T. A. *Macromolecules* **1994**, *27*, 449. (c) Grest, G. S. *Macromolecules* **1994**, *27*, 3493.

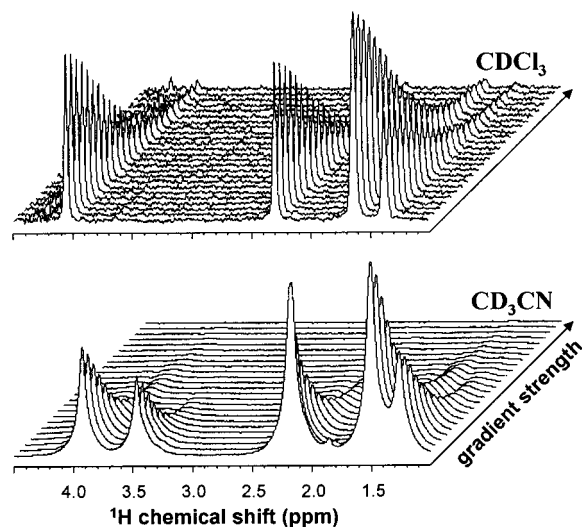


**Figure 6.** Stacked plot  $^1\text{H}$  NMR spectra of star polymer **3b** in  $\text{CDCl}_3$  (top) and  $\text{CD}_3\text{CN}$  (bottom) acquired with increasing gradient strength at  $298 \pm 1$  K.

to be 8.6 nm using eq 1, where  $\kappa^2$  is the orientation factor,  $J$  is

$$R_0 = \sqrt[6]{\frac{0.5291\kappa^2 J}{n^4 N_A}} \quad (1)$$

the overlap integral of the fluorescence intensity of the donor and the molar extinction coefficient of the acceptor normalized by the frequency expressed in wavenumbers,  $n$  is the index of refraction of the solvent, and  $N_A$  is Avogadro's constant.<sup>15b</sup> This suggests a diameter of **3d** in  $\text{CHCl}_3$  or toluene on the order of 18–20 nm. This value provides a reasonable explanation of why our attempts to directly obtain molecular size data by light scattering were not successful, since reliable data can usually only be obtained if the diameter of the investigated molecule is at least 1/20 of the wavelength of the laser (488 nm) used, i.e., at least 25 nm.<sup>29</sup>

**PGSE NMR Experiments.** In addition to its conventional role of providing detailed information about the local electronic environment of a molecule, NMR also represents a powerful tool for the study of overall molecular properties. Since sizes and shapes of molecular objects are related to friction factors for reorientational and translational motion, a correlation with nuclear relaxation rates is possible. Translational motion can effectively be studied by NMR using PGSE methods,<sup>30</sup> relating signal intensities to diffusion rates and therefore enabling the resolution of molecular dimensions in solution. With regard to nonbiological macromolecules, PGSE NMR has mainly been applied to the study of surfactant systems and polymer mixtures.<sup>30b</sup> Surprisingly in view of its great potential, the use of this method to study branched polymer architectures has so far been rather limited.<sup>31</sup> In our case, PGSE NMR represents

(29) (a) *Light Scattering from Polymer Solutions*; Huglin, M. B., Ed.; Academic Press: New York, 1972. (b) Wyatt, P. J. *Anal. Chim. Acta* **1993**, 272, 1 and references therein.

(30) Representative reviews include: (a) Johnson, C. S., Jr. *Prog. Nucl. Magn. Reson. Spectrosc.* **1999**, 34, 203. (b) Söderman, O.; Stilbs, P. *Prog. Nucl. Magn. Reson. Spectrosc.* **1994**, 26, 445. (c) Stilbs, P. *Prog. Nucl. Magn. Reson. Spectrosc.* **1987**, 19, 1. (d) Price, W. S. *Concepts Magn. Reson.* **1998**, 10, 197. (e) Price, W. S. *Concepts Magn. Reson.* **1997**, 9, 299.

(31) (a) Young, J. K.; Baker, G. R.; Newkome, G. R.; Morris, K. F.; Johnson, C. S., Jr. *Macromolecules* **1994**, 27, 3464. (b) Ihre, H.; Hult, A.; Söderlind, E. *J. Am. Chem. Soc.* **1996**, 118, 6388. (c) Valentini, M.; Pregosin, P. S.; Rügger, H. *Organometallics* **2000**, 19, 2551.

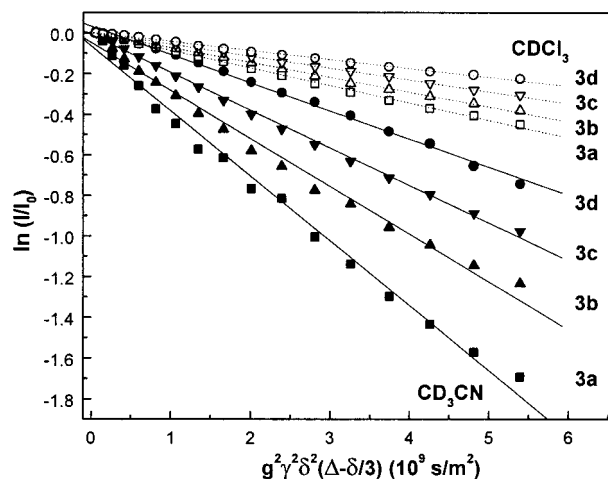


**Figure 7.** Plot of polymer peak area versus  $g^2\gamma^2\delta^2(\Delta - \delta/3)$  and linear fit for star polymers **3** in  $\text{CDCl}_3$  (open symbol, dotted lines) and  $\text{CD}_3\text{CN}$  (solid symbols, solid lines) at  $298 \pm 1$  K.

an ideal opportunity to study the effect of chain length as well as solvent on the actual size of the star polymers.

When a pulse sequence producing a spin-echo is repeated under conditions of increasing gradient strength, the observed signal intensities will decrease depending on the diffusion rate of the corresponding spin-labeled species. In this process the gradient encodes the spatial location of the observed molecule, similar to magnetic resonance imaging (MRI). Employing such experimental setup, star polymers **3a–d** were measured in  $\text{CDCl}_3$  and  $\text{CD}_3\text{CN}$ , respectively. Figure 6 shows two representative 2D NMR spectra, displaying chemical shift in one dimension and gradient strength, which is correlated to molecular diffusion and therefore size, in the other dimension. Depending on the solvent, the same polymer sample exhibits a distinctly different decay behavior. As a result of a larger diffusion coefficient, which in turn has its origin in a smaller size of the diffusing object, decay is faster in a bad solvent ( $\text{CD}_3\text{CN}$ ) than in a good solvent ( $\text{CDCl}_3$ ).

Quantitative analysis was accomplished by linear regression of the Stejskal–Tanner equation<sup>32</sup> (eq 2), where  $g$  is the gradient

$$I = I_0 e^{g^2\gamma^2\delta^2(\Delta - \delta/3)D} \quad (2)$$

strength,  $\gamma$  is the gyromagnetic ratio,  $\delta$  is the duration of gradient pulse,  $\Delta$  is the delay between consecutive gradient pulses, and  $D$  is the diffusion coefficient (Figure 7).<sup>33</sup>

From the obtained diffusion coefficients, the hydrodynamic radii  $R_H$  were estimated using the Stokes–Einstein equation (eq 3), where  $k_B$  is the Boltzmann constant,  $T$  is the absolute

$$R_H = \frac{k_B T}{6\pi\eta D} \quad (3)$$

temperature, and  $\eta$  is the viscosity of the solvent. The results clearly reflect the dependence of size and therefore site-isolation on chain length and solvent (Table 2). In both solvents the increasing DP corresponds to an increase in  $R_H$  giving rise to a “thicker” polymer shell around the core. In comparison to the

(32) Stejskal, E. O.; Tanner, J. E. *J. Chem. Phys.* **1965**, 42, 282.

(33) Although the investigated system is not monodisperse, satisfactory data ( $R > 0.99$ ) were obtained using a linear regression procedure. Presumably, the low polydispersity ( $\text{PDI} = 1.10\text{--}1.20$ ) and the high sphericity contribute to a narrow diffusion coefficient distribution. For details about polydisperse samples consult: (a) Reference 30. (b) Chen, A.; Wu, D.; Johnson, C. S., Jr. *J. Am. Chem. Soc.* **1995**, 117, 7965.

**Table 2.** Diffusion Coefficient  $D$  and Hydrodynamic Radii  $R_H$  of Star Polymers **3a–d** in  $\text{CDCl}_3$  and  $\text{CD}_3\text{CN}$ 

solvent	polymer	$D$ ( $\text{m}^2/\text{s}$ )	$R_H$ (nm)
$\text{CDCl}_3$	<b>3a</b>	$8.62 \times 10^{-11}$	4.7
	<b>3b</b>	$7.31 \times 10^{-11}$	5.5
	<b>3c</b>	$5.86 \times 10^{-11}$	6.9
	<b>3d</b>	$4.40 \times 10^{-11}$	9.2
$\text{CD}_3\text{CN}$	<b>3a</b>	$3.20 \times 10^{-10}$	2.0
	<b>3b</b>	$2.36 \times 10^{-10}$	2.7
	<b>3c</b>	$1.85 \times 10^{-10}$	3.4
	<b>3d</b>	$1.39 \times 10^{-10}$	4.6

good solvent, the poor solvent leads to largely reduced sizes indicating a collapse of the poly( $\epsilon$ -caprolactone) backbone around the core unit leading to a more densely packed shell. These results are in good agreement with the FRET studies described above. For instance, the  $R_H$  and  $\Phi_{\text{FRET}}$  values of **3a** in  $\text{CDCl}_3$  and **3d** in  $\text{CD}_3\text{CN}$  are comparable. Furthermore, the size of **3d** in  $\text{CDCl}_3$  as measured by PGSE NMR agrees well with the calculated Förster radius (vide supra) validating the assumption that the terminal ends are close to the periphery in the investigated polymer architectures.<sup>34</sup>

**Solvatochromic Probes.** In an alternative approach to study core isolation that does not involve porphyrin chromophores, star polymers **7a–d** and **8a–d** with a pyrene core were investigated as solvatochromic probes of their own core environment. Pyrene itself has been used extensively to help determine local environments since the vibrational fine structure of its fluorescence spectrum, namely the ratio of the  $I_1$  peak (0–0 band) and the  $I_3$  peak (0–2 band), is very sensitive to solvent polarity due to vibronic coupling (Ham effect).<sup>35</sup> With increasing polarity of the probe's microenvironment, the  $I_1:I_3$  ratio increases since the  $I_1$  band is markedly enhanced whereas the  $I_3$  band remains unaffected. In addition, pyrene can be used to study aggregation phenomena due to its characteristic excimer emission.<sup>36</sup>

As expected, when substitution is introduced  $r$  to attach the initiating functional groups, the pyrene moiety becomes less sensitive to changes in solvent polarity. The decreased probe sensitivity is not a result of the lowered symmetry of the system, but instead it derives from the introduction of the nearby carbonyl functionality, which presumably interferes with the vibronic coupling mechanism.<sup>37</sup> This substitution also prevents excimer formation, since even at relatively high concentrations of approximately 0.5 mM no excimer emission could be detected. However, when solvents such as toluene and DMSO were employed, representing extremes in polarity, a clear trend could be deduced from the  $I_1:I_3$  ratios (Figure 8).

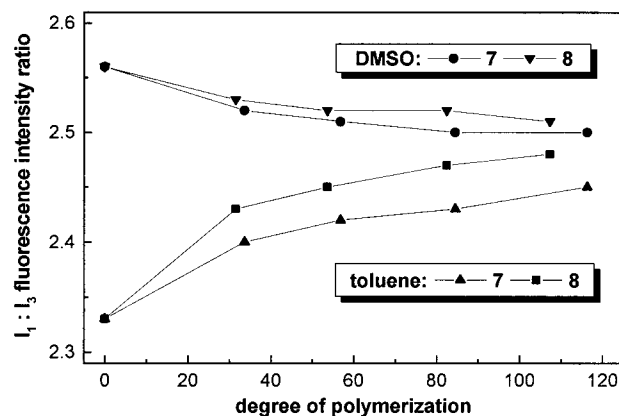
In agreement with the experiments described above, a significant chain length dependence on core isolation is found. With increasing DP, the local environment around the core

(34) The theoretical maximum radius assuming a fully extended conformation was estimated using molecular modeling that predicts a length of  $\sim 8.6$  Å for each monomer repeat unit. Therefore, polymer **3d** (DP = 50) would have a theoretical maximum radius of approximately 44 nm, i.e.,  $50 \times 8.6$  Å +  $1/2$  core size ( $\sim 10$  Å). The measured radius of 9.2 nm (Table 1) is much smaller, presumably due to substantial participation of random coil conformations.

(35) (a) Kalyanasundaram, K. *Photochemistry in Microheterogeneous Systems*; Academic Press: London, 1987; Chapter 2, p 36. (b) Kalyanasundaram, K. In *Photochemistry in Organized and Constraint Media*; Ramamurthy, V., Ed.; VCH: Weinheim, 1991; p 39.

(36) (a) Selinger, B. K.; Watkins, A. R. *Chem. Phys. Lett.* **1978**, *56*, 99. (b) Infelta, P. P.; Grätzel, M. *J. Chem. Phys.* **1979**, *70*, 179. (c) Atik, S. S.; Nam, M.; Singer, L. A. *Chem. Phys. Lett.* **1979**, *67*, 75.

(37) This can be shown by a comparison of the changes in  $I_1:I_3$  ratio ( $\Delta_{I_1:I_3}$ ) when going from acetonitrile to  $\text{CHCl}_3$ : for pyrene  $\Delta_{I_1:I_3} \approx 0.5$ , for initiators **5** and **6**  $\Delta_{I_1:I_3} \approx 0.1$ , whereas for 1-pyrenemethanol  $\Delta_{I_1:I_3} \approx 0.6$ .

**Figure 8.** Solvatochromic probing using the  $I_1:I_3$  fluorescence intensity ratio in two series of pyrene core star polymers having 2 arms (**7a–d**) and 4 arms (**8a–d**) in toluene and DMSO.

approaches a polarity reflecting that of the poly( $\epsilon$ -caprolactone) shell, which is more polar than toluene but less polar than DMSO. As observed with the FRET measurements (Figure 4), the response to a change in chain length is more pronounced in the good solvent, providing further evidence in support of solvation-induced site encapsulation. Furthermore, the change in the number of arms, going from **7a–d** to **8a–d** (2 vs 4 arms), contributes more to site isolation than the change from **1a–d** to **2a–d** (8 vs 16 arms), especially when the polymer is extended (good solvent). This is not surprising since the shape differences ( $\Delta\delta$ )<sup>18</sup> between the 2-arm star ( $\delta = 0.53$ )<sup>19</sup> and the 4-arm star ( $\delta = 0.27$ ) are more pronounced than those for the 8-arm star ( $\delta = 0.14$ ) and 16-arm star ( $\delta = 0.07$ ), recalling that  $\delta = 0$  for a sphere (vide supra).

## Conclusions

The construction of star polymers via ring-opening polymerization of  $\epsilon$ -caprolactone using functional dendritic initiators has been demonstrated to be an efficient route for the encapsulation of active core functionalities. While this approach lacks the precision of dendrimer encapsulation,<sup>3</sup> it is synthetically simpler providing access to a larger range of sizes and allowing the products to be easily purified by precipitation. Moreover, this route seems to be fairly general, since in principle any functional core carrying phenol or alcohol functionalities (or conceivably amines) could be encapsulated using similar chemistry. The possibility of post-modification affords access to a wide variety of materials, which may be used to probe the effect of variables such as chain length, number of arms, or solvent on core isolation. Using three different types of assays, namely fluorescence quenching, FRET, and solvatochromic probes, it has been shown that core encapsulation is mainly dependent on DP with only minor contributions arising from the number of arms. In addition, poor solvents seem to further increase the degree of site isolation due to a structural collapse of the polymer backbone giving rise to a more dense shielding around the core unit. This solvation-induced encapsulation effect and the chain length dependence are supported by PGSE NMR experiments that allow for direct determination of the molecular sizes of the polymers in different solvents. FRET as well as PGSE NMR have been shown to be particularly useful techniques to study the dynamics of star polymers in solution. These studies concerned with the general principles of site-isolation and its practically useful realization will ultimately lead to the design of future functional materials.

**Acknowledgment.** Henrik Ihre is acknowledged for his help in the early stages of the project as well as Seth Bush and Rudi Nunlist for their invaluable help with the PGSE NMR experiments. Financial support from the AFOSR-MURI program and the National Science Foundation (NSF-DMR 9816166) is acknowledged with thanks.

**Supporting Information Available:** Experimental details and chemical characterization data (PDF). This material is available free of charge via the Internet at <http://pubs.acs.org>.

JA003304U